Thermal stresses in a Drucker Prager elastoplastic hollow cylinder subjected to thermal shock: influence of material and structure parameters

Nicolas Schmitt, E. Baquet, P. Guillo, Eric Blond

Proceedings of the Seventh International Congress on Thermal Stresses, June 4 -7, Taipei TAIWAN (2007)
Vol. 2, pp 771-774, Editors C.K. Chao and C.Y. Lin, Publisher NTUST, Taipei (Taiwan)

THERMAL STRESSES IN A DRUCKER PRAGER ELASTOPLASTIC HOLLOW CYLINDER SUBJECTED TO A THERMAL SHOCK: INFLUENCE OF MATERIAL AND STRUCTURE PARAMETERS

N. SCHMITT[1,a], E. BAQUET[1], P. GUILLO[2], E. BLOND[3]

[1]*LMT-Cachan (ENS de Cachan, CNRS, University Paris 6)*
61, avenue du Président Wilson 94235 Cachan (France)
[2]*VESUVIUS France*
68 rue P. Deulon 59750 Feignies (France)
[3]*LMSP (CNRS, ENSAM Paris, University Orléans)*
8, rue Léonard de Vinci 45072 Orléans (France)

The thermomechanical behavior of a hollow cylinder subjected to a sudden rise of its inner temperature is examined. An elastoplastic linear Drucker-Prager model is identified with data from tensile and compressive tests made on alumina graphite refractories. The role of material non linearity on thermal shock resistance is studied thanks to finite element simulations. It is shown that the energy dissipated by plasticity is a more sensitive material parameter for the design of components in comparison to the thermal stresses usually chosen.

Keywords: *thermal shock, hollow cylinder, Drucker-Prager model, parametric study*

1 Introduction

Alumina graphite refractories are ceramics with good chemical and mechanical resistances at high temperature up to 1600-1700°C [1]. They are widely used in steel industries. The manufacturers propose a wide range of chemical composition of the material depending on the severity of the environment of refractory pieces. For this reason, it is not possible to identify the thermomechanical behavior of each material at high temperature accurately, so that empirical rules are often used for design. In particular, Kingery's shock resistance [2] is a popular criterion used for the classification of the refractories but it is not well adapted for ceramics exhibiting a non linear behavior.

The role of the nonlinearity of the mechanical behavior of the material on the thermal shock resistance is analyzed. A particular attention is paid to the variability of the material parameters considering variations up to ±20% of the medium-value. In order to catch the main features a simplified non linear model is used that takes into account both apparent plasticity and asymmetric tensile-compressive behavior. Results of the identification and numerical simulations of a tube subjected to a thermal shock are shown in the following sections.

2 Identification of Drucker-Prager's constitutive equations for alumina graphite refractories

2.1 Microstructure of the refractory

Alumina Graphite Refractories (AGR) are heterogeneous ceramics with a high porosity (16-20%).

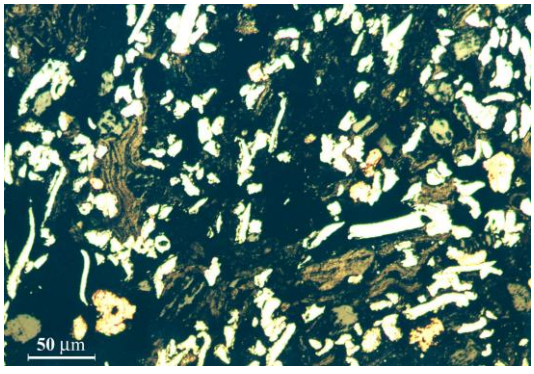

Figure 1: Micrograph of an AGR

They contain coarse and fine oxide aggregates (70-80% in weight) with size ranging from 10 µm to 500 µm and a carbon phase (20-30% in weight) (Fig. 1). Alumina oxides are mainly used but other oxides like

[a] Associate Professor, Nicolas.Schmitt@lmt.ens-cachan.fr

zirconia, mullite… Metal particles are sometimes introduced to improve some properties. The carbon phase is composed of both an organic resin fired at high temperature to obtain a rigid carbon skeleton and graphite flakes (100-900 μm length, 15-100 μm width) to improve the resistance to thermal shock and the chemical resistance.

These ceramics exhibit a strong non linear behavior (Fig. 2). The carbon skeleton and the graphite flakes are at the origin of the non linear behavior of the ceramics. Indeed, many cracks are observed in the carbon phase occurring during the manufacturing process (pressing and firing) and the interface between the carbon matrix and the grains are partially debonded.

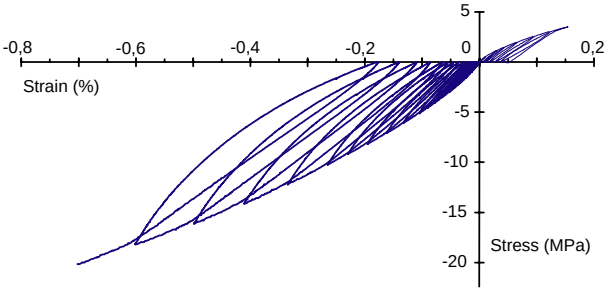

Figure 2: Typical results of compressive and tensile tests at room temperature [3]

The refractory has both a higher resistance and a higher ductility in compression than in tension and there exists a hysteretic behavior during unloading and reloading due to opening and closing of the cracks. The levels of the mechanical properties depend on both the chemical composition and the temperature. When the temperature increases, the strength decreases whereas the ductility becomes higher.

2.2 Constitutive equations

Experimental data are used to identify the linear isotropic elastic and linear original Drucker-Prager plastic model [4]. This model allows with a limited number of parameters to catch the main features of the mechanical behavior. But the damage and the hysteretic behavior are not taken into account. The main equations are shown in Eqs. 1-6.

An additive strain rate decomposition is assumed

$$d\varepsilon = d\varepsilon^{el} + d\varepsilon^{in} + d\varepsilon^{th} \tag{1}$$

where ε, ε^{el}, ε^{in} and ε^{th} are respectively the total, the elastic, the inelastic and the thermal strain tensors.

The thermal strain reads

$$\varepsilon^{th} = \alpha(T - T_i)I \tag{2}$$

where α is the thermal expansion coefficient, T and T_i respectively the temperature and the initial temperature and I the unit tensor.

The elastic law is given by

$$\sigma = K \cdot \left(\varepsilon - \varepsilon^{in} - \varepsilon^{th}\right) \tag{3}$$

where σ is the Cauchy stress tensor and K the elastic matrix.

The yield function of the linear Drucker-Prager law and the yield criterion are given respectively

$$F(\sigma_H, \sigma_{eq}) = \sigma_{eq} - \sigma_H \times \tan\beta - d(\bar{\varepsilon}^{in})$$
$$F(\sigma_H, \sigma_{eq}) = 0 \tag{4}$$

where σ_H is the hydrostatic pressure, σ_{eq} the equivalent Mises stress, β the friction angle.

The dependence of d on the equivalent inelastic strain $\bar{\varepsilon}^{in}$ permits to account for isotropic hardening.

The flow potential is given by

$$G(\sigma_H, \sigma_{eq}) = \sigma_{eq} - \sigma_H \times \tan\psi \tag{5}$$

where ψ is the dilation angle. We assume herein fully associated model of Drucker-Prager with $\psi = \beta$ [4].

When the yield criterion is reached, the flow rule is defined as

$$\varepsilon^{in} = \lambda \frac{\partial G(\sigma_H, \sigma_{eq})}{\partial \sigma} \tag{6}$$

2.3 Identification

In this model, the parameters E, ν, (Young's modulus and Poisson's ratio) and α are respectively: E = 9 GPa, ν = 0.2 and $\alpha = 3\times10^{-6}$ °C^{-1}.

β and d are identified respectively considering that

$$\beta = \tan^{-1}\left(\frac{3(\sigma_c - \sigma_t)}{\sigma_c + \sigma}\right) \tag{7}$$

and

$$d(\bar{\varepsilon}^{in}) = \frac{\sigma_t(\varepsilon_{11}^{in})}{3}\tan\beta \tag{8}$$

β = 64.8° and d is identified with the tensile curve.

The model fits the tensile curve with a good accuracy but as isotropic hardening is used, the hardening in compression is higher than that observed. Nevertheless, this is not a problem because the main observed failures in refractory pieces are caused by excessive tensile stress.

3. Simulations of a hollow cylinder

3.1 Model

Lets consider a hollow cylinder with an inner radius R_i = 35 mm and an outer radius R_e = 50 mm, initially at room temperature T_0 = 20°C, subjected to convective heat flux

$$\phi_i = h_i(T_i - T_{is}) \tag{9}$$

$$\phi_e = h_e(T_e - T_{es}) \tag{10}$$

h_i and h_e are respectively the convection coefficient at the inner and outer surface (h_i = 1500 W.m^{-2}, h_e = 20 W.m^{-2}) and T_i and T_e the inner and outer temperature (T_i = 1500 °C, T_e = 150 °C).

This problem is representative of a Ladle Shroud (LS) connecting the ladle with the tundish in continuous casting process [3]. The tube protects the steel stream against oxidation from the atmosphere and minimizes steel splashing.

Simulations are made with the finite element code ABAQUS [5]. The tube is meshed with axisymmetric elements CAX8RT considering generalized plane strain. Fully coupled thermal stress analysis is made. The time integration is made using the backward difference algorithm and the non linear equations are solved by a modified Newton method.

3.2 Results for the reference case

The difference in temperature $\Delta T = T(r,t)-T_m(t)$ at the inner surface $r=R_i$ and the outer surface $r=R_e$ and the average temperature $T_m(t)$ is shown in Fig. 3. ΔT is responsible of the development of thermal stresses in the LS.

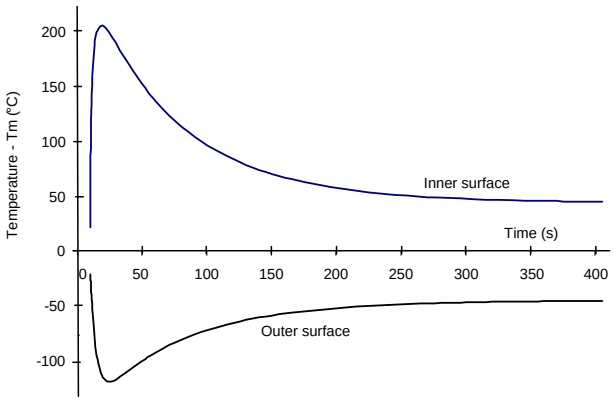

Figure 3: Temperature minus average temperature change versus time in the tube (thickness 15 mm)

ΔT reaches about +210°C at the inner surface and -120°C at the outer surface before its magnitude decreases. The time at which $|\Delta T_{max}|$ is maximum is close to the time where failure of the LS sometimes occurs. Kingery's criterion ΔT_c

$$\Delta T_c = \frac{\sigma^r}{E\alpha}(1+\upsilon) \qquad (11)$$

allows an estimation of the maximum temperature that the material can withstand under a hard thermal shock. It is equal respectively to ΔT_c = 160°C at radius R_e with tensile strength σ^t = 3.6 MPa and ΔT_c = 933°C at R_i with compressive strength σ^c = 21 MPa. Consequently failure is predicted at the cold face of the tube with this criterion. This seldom occurs for this tube.

Fig. 4 shows the evolution of the axial stress at several depths during the first 200 seconds. When the temperature increases, inelastic strains occur first at the outer surface. An inelastic zone spreads several mm-depth as long as the stress has not decreased enough, then it is stopped. Inelastic strains develop also at the inner surface a bit later, but due to the higher resistance in compression the zone is not as large as at the outer zone.

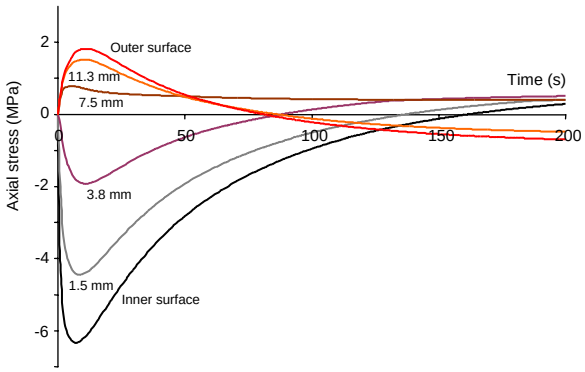

Figure 4: Axial stress versus time at different depths (tube thickness 15 mm)

The results (Figs. 3-4) agree with the in-situ observations: no failure of the LS is detected several ten seconds after the start of the thermal shock.

3.3 Influence of the material parameters

To take into account the variability of the material parameters, a parametric study was made by considering a ±20% variation of properties compared with the reference values used for the previous study. The thermal expansion coefficient is the most sensitive parameter. Its influence on several variables is shown in Fig. 5 for the outer surface (the critical one). The values of these variables are computed at the time where the temperature difference is the highest in the zone studied.

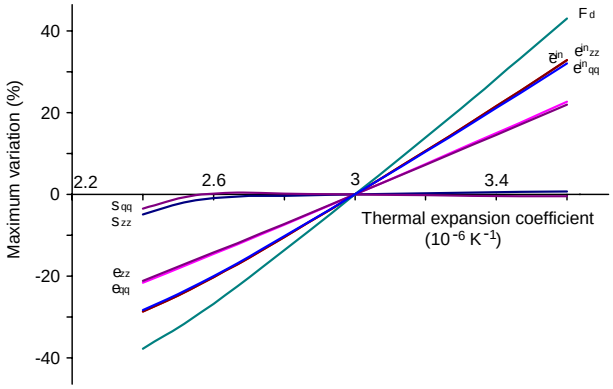

Figure 5: Maximum variation of variables versus coefficient of thermal expansion α at the outer surface (tube thickness 15 mm)

The thermal stresses are less sensitive to the variability of α when the inelastic strains and the energy dissipated by "plasticity" $\Phi_d = \int \sigma \cdot \dot{\varepsilon}^{in} dt$ are sensitive. Consequently, the estimation of the thermal stresses is not enough to establish a criterion for the thermal shock.

One can remark that for associate Drucker-Prager law either $\bar{\varepsilon}^{in}$ or Φ_d can by used as equivalent material parameters to measure the intensity of the thermal shock, but the last parameter is more sensitive.

As the product of Young's modulus and the thermal expansion coefficient is very important for the thermal shock resistance (see Eq. 11), simulations were made in which both values varied as $E=E_o\times(1+\eta)$ and $\alpha = \alpha_o\times(1-\eta)$ with $\eta \in [-0.2, 0.2]$. The results are shown in Fig. 6 for several parameters.

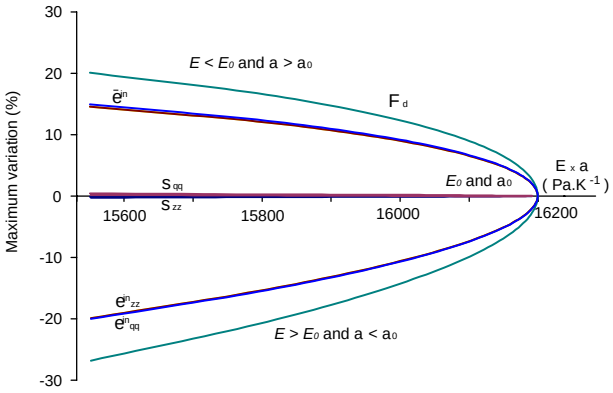

Figure 6: Maximum variation of variables versus the coefficient of thermal expansion at the outer surface (tube thickness 15 mm)

Again, the thermal stresses are less sensitive to the variability of both E and α (±20%) because the product varies less (≈4%). This agrees with the Kingery's thermal shock criterion (Eq. 11). But at the same time, one observes a great variation of both the inelastic strain and the intrinsic dissipation. The influence of E and α is different. Higher values of the analyzed parameters are obtained when α increases and E decreases than for the other case. Consequently, to decrease the risk of failure, it is more interesting to reduce the thermal expansion coefficient than Young's modulus.

3.4 Influence of the structural parameters

Let us now examine the effect of the thickness of the tube. To agree with typical geometry of LS produced by the manufacturer, the inner radius varies also when the thickness e varies

$$R_i^{-1} = 6.7 + 0.336/e \quad \text{(m)} \qquad (12)$$

An increase of e results in a small variation of the stresses at the outer surface (less than 10 % when e varies from 10 to 40 mm). But a sensitive variation of the stresses exists at the inner surface: the compressive stress varies from -6 MPa for e = 10 mm up to -12 MPa for e = 40 mm. This suggests that a thin tube has a better thermal shock resistance than a thick tube. In practice, this is not observed. The manufacturer prefers to use thicker tube, although it is more expansive.

To explain this paradox, let us examine the evolution of the intrinsic dissipation with time at the outer surface for several thicknesses (Fig. 7).

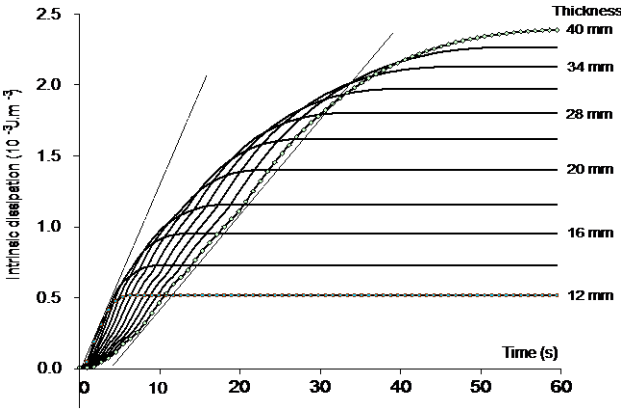

Figure 7: Change of the intrinsic dissipation with time at the outer surface for several tube thicknesses

The maximum intrinsic dissipation obtained for the tensile test Φ_{dT}^{max} = 3000 J.m^{-3} is higher than the maximal value observed for the tested geometry. Consequently, there exists no risk of failure of the tube even for e = 40 mm. With regard to previous remarks, thick tubes have a greater risk of failure than thin tube. However, during the first tens seconds, the maximum rate of Φ_d is lower for thick tubes than for thin tubes. Perhaps this could explain that thicker tubes are more resistant to thermal shock than thinner tubes. This point is studied currently.

References

[1] Lee, W.D., Moore, R.E, Evolution of in situ refractories in the 20th century, *J. Am. Ceram. Soc.*, **81** [6], 1381-1410, 1998.

[2] Kingery, W.D., Factors affecting thermal stress resistance of ceramic materials, *J. Am. Ceram, Soc.*, **38** [1], 3-15, 1955.

[3] Peruzzi, S., Simulation numérique du comportement thermomécanique de pièces réfractaires de coulée continue, *Ph.D. dissertation, University of Limoges*, France, (in French), 2000.

[4] Drucker, D.C., Prager W., Soils mechanics and plastic analysis or limit design, *Quartely of applied mathematics*, vol. 10, 157-165, 1952.

[5] Hibbitt, Karlson, Sorensens, Abaqus calculation code, version 6.3, HKS, Inc, Pwtucket, USA, 2006.